PCCP

Accepted Manuscript

This article can be cited before page numbers have been issued, to do this please use: S. Seng, A. L. Picone, Y. B. Bava, L. C. Juncal, M. Moreau, R. Ciuraru, C. George, R. M. Romano, S. Sobanska and Y. A. Tobon, *Phys. Chem. Chem. Phys.*, 2018, DOI: 10.1039/C7CP08658J.

This is an Accepted Manuscript, which has been through the Royal Society of Chemistry peer review process and has been accepted for publication.

Accepted Manuscripts are published online shortly after acceptance, before technical editing, formatting and proof reading. Using this free service, authors can make their results available to the community, in citable form, before we publish the edited article. We will replace this Accepted Manuscript with the edited and formatted Advance Article as soon as it is available.

You can find more information about Accepted Manuscripts in the author guidelines.

Please note that technical editing may introduce minor changes to the text and/or graphics, which may alter content. The journal's standard Terms & Conditions and the ethical guidelines, outlined in our author and reviewer resource centre, still apply. In no event shall the Royal Society of Chemistry be held responsible for any errors or omissions in this Accepted Manuscript or any consequences arising from the use of any information it contains.

ROYAL SOCIETY OF CHEMISTRY

rsc.li/pccp

View Article Online
DOI: 10.1039/C7CP08658J

Journal Name

ARTICLE

Photodegradation of Methyl Thioglycolate Particles as a Proxy for Organosulphur Containing Droplets

Received 00th January 20xx,
Accepted 00th January 20xx

DOI: 10.1039/x0xx00000x

www.rsc.org/

Samantha Seng,[a] A. Lorena Picone,[b] Yanina B. Bava,[b] Luciana C. Juncal,[a,b] Myriam Moreau,[a] Raluca Ciuraru,[c‡] Christian George,[c] Rosana M. Romano,[b] Sophie Sobanska,[a†] and Yeny A. Tobon[a*]

Understanding the formation and transformation of sulphur-rich particles is of prime importance since they contribute to the global atmospheric sulphur budget. In this work, we performed a series of experiments on a photoactive organosulphur compound namely, methyl thioglycolate, as a model of an organosulphur species of marine origin. By investigating the photoproducts within levitated droplets, we showed that elemental sulphur (α-S_8) and sulphate (SO_4^{2-}) can be photochemically generated at the gas-liquid interface by heterogeneous interaction with gaseous O_2 and H_2O. These results demonstrate that the surface of levitated droplets facilitate the oxidation of methyl thioglycolate in the dark, while illumination is necessary to produce the oxidation in bulk experiments.

1. Introduction

Sulphur is an abundant element in the environment and its cycle is one of Earth's fundamental geochemical cycles. In the atmosphere, sulphur is present in various oxidation states, in both gas and condensed phases. The most abundant gaseous S-containing species is sulphur dioxide (SO_2) which arises from a variety of natural and anthropogenic sources. The oxidation of SO_2 in air leads to the formation of sulphuric acid as well as sulphate-containing particles through a combination of gas and aqueous processes, with some contribution from heterogeneous chemistry.[1] Sulphate-containing particles contribute significantly to the global mass fraction of atmospheric submicrometre aerosols[2] and have recognized impacts on human health, and the climate. Although the combustion fossil fuels account for the major source of SO_2 in urban and industrial environments,[3] the oxidation of reduced sulphur compounds (i.e., OCS, H_2S, CS_2 and dimethyl disulphide –DMS-) account for much of the SO_2 observed in the remote troposphere and stratosphere.[4]

DMS is of a particular interest since it is the main reduced sulphur-rich compound produced in oceanic areas.[5] The major source of DMS in marine environment is dimethylsulphoniopropionate ($(CH_3)_2S^+CH_2CH_2C(O)O^-$, DMSP), which is naturally produced by algae and aquatic plants. However, other organosulphur compounds such as methanethiol, 3-methylmercaptopropionate and 3-mercaptopropionate[6-9] are also produced by related degradation pathways of DMSP, and have a sufficiently low vapour pressure to likely contribute to the global dissolved organic sulphur (DOS) budget in oceans.[10] The emission of primary marine particles containing DOS from biogenic sources has been largely ignored. However, a recent work has demonstrated the presence of DOS in primary marine aerosols.[11] Then, DOS species may be emitted into the atmosphere as part of sea salt particles, through bubble bursting and wind action. Once in the atmosphere, organosulphur droplets are subject to atmospheric chemical and photochemical aging processes. Although the (photo)reactivity of sulphur compounds in the atmosphere is complex and has been widely explored in the gaseous phase,[12,13] (photo)transformation of particles containing dissolved organosulphur compounds has been neglected.[14,15] Recently, Gaston et al.[11] measured primary marine particles containing reduced sulphur, detected as elemental sulphur ions, in seven field campaigns conducted in various marine environment. Strong diurnal profile of these particles was explained by the marine biogenic activity and the rapid destruction of the sulphur-containing compounds during the daytime due to photolysis.

In this work, we have studied the photoreactivity of pure and aqueous methyl thioglycolate –MTG, $CH_3OC(O)CH_2SH$–, a photoactive organosulphur compound[16] used as a proxy for DOS. We have reported its photoreactivity, on single droplets, using an acoustic levitation system.[17] Indeed, studying the processes in aerosols, at the single particle scale, is an added value to better understand the physicochemical mechanisms intervening in complex heterogeneous atmospheric processes.[18-22] Complementary experiments in bulk and at the

[a] Laboratoire de Spectrochimie Infrarouge et Raman, UMR CNRS 8516, Université Lille 1 Sciences et Technologies, Bât, C5, 59655 Villeneuve d'Ascq Cedex, France. E-mail: yeny.tobon-correa@univ-lille.fr.
[b] CEQUINOR (UNLP, CCT-CONICET La Plata). Departamento de Química, Facultad de Ciencias Exactas, Universidad Nacional de La Plata. Blvd. 120 N° 1465, La Plata (CP 1900), Argentina.
[c] Univ Lyon, Université Claude Bernard Lyon 1, CNRS, IRCELYON, F-69626, Villeurbanne, France.
† Present address: Institut des Sciences Moléculaires, UMR CNRS 5255, 351 cours de la Libération, 33405 Talence, Cedex, France.
‡ Present address: UMR ECOSYS, INRA, AgroParisTech, Université Paris-Saclay, 78850 Thiverval-Grignon, France

View Article Online
DOI: 10.1039/C7CP08658J

air-solution interface were conducted to highlight single particle-only process. We showed that elemental sulphur and sulphate can be formed on the droplet surface by photolysis of the organosulphur compound in the presence of gaseous oxygen and water. In addition, the surface of the droplet played an important role in the reactivity of MTG and triggered its oxidation, which alters the progress of the reaction and the final products.

2. Experimental methods

2.1. Chemical reagents

Commercial samples of methyl thyoglycolate –MTG, $CH_3OC(O)CH_2SH$– (Alfa Aesar) were used without further purification. Ultrapure deionized water (Milli-Q™, 18 MΩ) was used to prepare aqueous solutions of MTG (0.3M).

2.2. Single levitated particle experiments

The levitation system was already described previously.[17] It consists in an acoustic levitator (APOS BA 10, Tec5, Germany) equipped with a homemade environmental cell coupled horizontally to a confocal Raman microspectrometer. The cell has four optics accesses and transparent quartz windows allowing exposure to UV-visible light and particle analysis. Two inlet/outlet valves for gas supplies can modify the environment inside the cell, including the relative humidity (RH).

Raman microspectrometry measurements of the levitated particles were performed with a LabRAM confocal spectrometer (Horiba Scientific, S.A). Spectra were recorded at a resolution of 4 cm^{-1}. The instrument was equipped with an Olympus BX40 microscope using a Nikon x50 objective (NA = 0.45; WD= 13.8 mm), and a He-Ne laser (λ= 632.8nm). The laser power on the droplet surface was limited to 0.6 mW (10% of full laser power). The lateral resolution was estimated ~ 2 µm and the depth of the laser focus to 16 µm with a Δz limit ≥ ± 3 µm. Thus, considering the volume probed by the laser beam, the analysed surface corresponds to a layer of a few microns. A high-speed high-resolution video camera CMOS monochrome (Basler Ace NIR, 2048 x2048 pixels) was also adapted to the Raman microscope allowing the visualisation of morphological changes on the surface of the particle before, during and after the irradiation of the particle with a resolution time of millisecond.

Microdroplets ranging from 35 to 80 µm were trapped by direct injection of a drop into the acoustic cavity under environmental conditions (20°C, 40-50 %RH). After trapping and Raman analysis of the single levitated particle, droplets were exposed to a broadband UV-vis light (300 ≤ λ ≤ 800 nm) from a Hg-Xe arc lamp, Hamamatsu, LC8 Lightningcure, 200 W (power on the droplet = 3.9 10^{-3} mW.µm^{-2}) equipped with a water filter to absorb infrared radiation and minimize any heating effect, or to a monochromatic radiation of 325 nm from a CW He-Cd laser (power on the droplet = 2.6 10^{-3} mW.µm^{-2}). Raman spectra of the levitated particle were recorded at different time of irradiation, with close attention to the decay of Raman bands of the initial compounds and to the appearance and subsequent behaviour of any new features. In order to compare the laser and lamp experiments, photon flux density at 325 nm was calculated from the power source data. In the case of the broadband lamp, a bandpass/single-band Semrock^M filter centred at 325 nm (FWHM = 1.2 nm) and corrected by the transmittance of the filter (85%) was used to obtain the photon flux density in the 325-nm region. The photon flux was 7.1 10^6 µmol.m^{-2}.s^{-1} and 9.8 10^3 µmol. m^{-2}.s^{-1} for the 325 nm-laser beam and the lamp in the 325-nm region, respectively.

2.3. Bulk experiments

Pure MTG and aqueous solutions of MTG (0.3M) were placed into a quartz reactor under constant stirring. Samples were exposed to broadband UV-vis light from a Hg-Xe arc lamp, Hamamatsu, LC8 Lightningcure, 200 W (300 ≤ λ ≤ 800 nm). The output of the lamp was limited by a water filter to absorb infrared radiation and minimize any heating effect. Chemical changes were followed by Raman microspectrometry.

2.4. Air/aqueous interface experiments

Air/aqueous interface photochemistry was performed in a quartz cell (2 cm diameter and 5 cm length) filled with 7 mL of mixtures (aqueous solutions of MTG, 0.3 M). The solutions were irradiated using a Xenon lamp, operating at 150 W (300 ≤ λ ≤ 800 nm) and 400 sccm of purified air was flowing through the quartz cell. A water filter was used in order to absorb infrared radiation and minimize any heating effects. The gas-phase products were investigated by proton transfer reaction mass spectrometry using a commercial SRI-PTR-ToF-MS 8000 (Selective Reagent Ionization Proton Transfer Reaction Time of Flight Mass Spectrometer) instrument from Ionic on Analytik GmbH (Innsbruck, Austria). The PTR-MS sampled continuously 50 sccm through 1.5 m of 6 mm (i.d.) polyether ether ketone (PEEK) tubing. Measurements were performed in H_3O^+ ionization mode at a drift voltage of 600 V, drift temperature of 60°C and a drift pressure of 2.25 mbar resulting in an E/N of 130 Td (1Td=$10^{-17}$$cm^2V^{-1}$), the spectra being collected at a time resolution of 2 min. The compounds concentrations have been calculated according to Cappellin *et al.*[23] and the same value of $k = 2\times10^{-9}$ cm^3s^{-1} was used for all masses.

3. Results and discussion

3.1. Single levitated particle experiments

Pure MTG. Levitated droplets of pure MTG, of around 80 µm of diameter, were obtained by direct injection into the acoustic cavity. Raman spectra of the levitated droplets, collected immediately after injection, mainly displayed the Raman bands characteristic of liquid MTG[24,25] and a very small peak around 510 cm^{-1} attributed to the S-S stretching mode of the disulphide derivative $[CH_3OC(O)CH_2S]_2$ (Dimethyl dithiodiglycolate –DMTG–)[26] that was present in the bulk

View Article Online
DOI: 10.1039/C7CP08658J
Journal Name ARTICLE

sample as an impurity since we did not purify the sample before experiments. As shown in the preliminary results,[17] in Figure 1, before irradiation, oxidation of MTG to its disulphide derivative was evidenced by the growth of the S-S stretching mode around 510 cm^{-1}, accompanied by the disappearance of the band near to 2568 cm^{-1}, belonging to the S-H stretching mode of the MTG. The chemical transformation occurred simultaneously with the decrease in the size of the droplet from 70 µm to 38 µm, revealed by the optical images (See Figure S1 of the Supporting Information). Some evaporation of MTG from the droplet surely caused the size reduction of the particle diameter (MTG vapour pressure = 10 mbar at 25 °C). As evidenced by Raman spectroscopy, oxidation of MTG into DMTG occurred within a few minutes after exposure to ambient O_2, and was assumed to be complete after 16 hours (Equation 1). Indeed, after 16 hours, no MTG was detected in the core of the droplet.

$$4\ CH_3OC(O)CH_2SH + O_2 \rightarrow 2\ [CH_3OC(O)CH_2S]_2 + 2\ H_2O \qquad (Eq.1)$$

The relative humidity inside the cell was observed to increase from 45 to 55 %RH mainly due to external RH variation during the experiment. Although some water is produced from the MTG oxidation reaction as showed in Equation 1, the very small quantity of water generated from the microdroplet would increase by less than 0.1% the %RH inside the 20-ml environmental cell.

Thus, single particle irradiation experiments were performed after the complete oxidation of MTG into DMTG. In a first experiment, the droplet was irradiated with broadband UV-vis light ($300 \leq \lambda \leq 800$ nm) from a Hg-Xe lamp . A second experiment was performed irradiating a droplet with a 325-nm monochromatic light emitted by a CW He-Cd laser was carried out. Changes in the Raman spectra were recorded as a function of irradiation time. The decay of the DMTG bands was accompanied by the appearance and the growth of new bands in the two experiments.

Figure 2 shows new bands at 153, 219, 468 and 475 cm^{-1} that appeared after 10 minutes of irradiation with the broadband UV-light. These bands are unambiguously attributed to the vibrational fundamental modes of elemental sulphur (α-S_8) by comparison with the well-known reported Raman spectra[27,28]. Only the bands of elemental sulphur dominated the Raman spectrum with almost total extinction of the disulphide bands after 90 minutes of photoprocess accompanied with a size reduction of the particle of about 22%. For longer exposure time, we did not observe any further changes in the Raman spectrum. However, when the laser beam was focalised deeper in the particle core, in the Z direction, some disulphide bands still remained in the spectra. Therefore, we hypothesized that phototransformation likely occurred on the droplet surface and elemental sulphur passivated the surface, preventing further any photooxidation.

The photoreaction rate coefficient of DMTG was deduced from the time resolved Raman spectra, by measuring the integrated area of the S-S stretching mode. Normalisation was carried out by performing the ratio between integrated area of the bands for each irradiation time (A) and the integrated area before irradiation (A_0). Considering the signal-to-noise ratio, using this method, we estimate an error of 10%. Consequently, by plotting the $\ln(A/A_0)$ as a function of the irradiation time, we have determined that disulphide photodegradation corresponds to a first order kinetics with a reaction rate coefficient (k_1) near to 4.0 10^{-2} min^{-1} and a lifetime (τ) of 25.0 min (See Figure S2 of the Supporting Information).

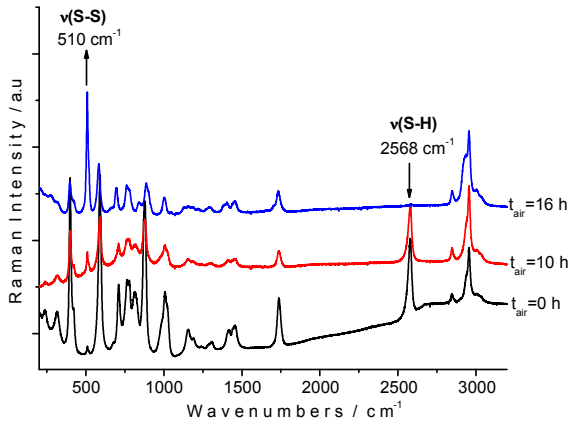

Fig. 1. Raman spectra of a levitated droplet initially containing methyl thioglycolate in the region of 200-3200 cm^{-1} before irradiation, immediately after injection (0h), and after 10 and 16 hours exposed to air.

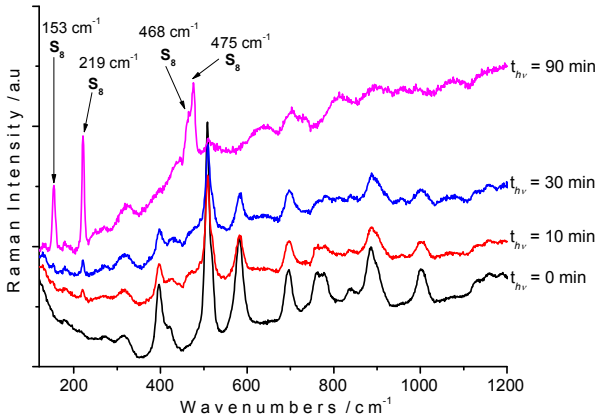

Fig 2. Raman spectra of a levitated droplet initially containing dimethyl dithioglycolate (Disulphide) in the region of 120-1200 cm^{-1}before and after 10, 30 and 90 minutes of irradiation with broadband UV-Vis light (300-800 nm)

In this experiment, the surface of the particle was mostly homogeneously irradiated and elemental sulphur was found regularly distributed on the particle surface. Evidently, other products were formed during the photoprocess but they have not been detected in the particle by Raman microspectroscopy. They were probably emitted into the gas phase.

Alternatively, as it is reported in our previous work,[17] when a particle is irradiated with a 325-nm laser, a very quick transformation is observed on the Raman spectra, with the simultaneous appearance of bands attributed to sulphate (SO_4^{2}) centred at 618 and 976 cm^{-1},[29] and bands attributed to elemental

View Article Online
DOI: 10.1039/C7CP08658J

sulphur (219, 468 and 475 cm^{-1}). DMTG photodegradation seemed to be faster using laser irradiation than in the broadband experiments, with an uncorrected k_2' at 0.28 min^{-1} that belongs to a lifetime (τ') of 3.6 min. The 325-nm laser provided higher energy and local photon flux density from a unique wavenumber than broadband UV-lamp, which produced local transformation on the droplet surface. As the laser photon flux density was higher than that obtained with the lamp (in the 325-nm region), the laser reaction rate coefficient (k_2') was corrected by a factor calculated from the laser/lamp photon flux ratio to get a corrected k_2 of 3.9 10^{-4} min^{-1} (τ = 2564 min) (Figure S2). The large reaction rate constant difference between both experiments ($k_1 \cong 100\ k_2$) suggested that the reaction was not only due to the 325-nm light absorption and that broadband light irradiation also played an important role in the photodegradation of the disulphide derivative.

By recording the Raman spectra on various points on the surface, perpendicularly to the laser beam irradiation, we probed sulphate ions and elemental sulphur products distribution on the particle surface (Figure 3a). The SO_4^{2-}/S_8 ratios were roughly estimated for each focal point by measuring the integrated area of the 976 and 219 cm^{-1} Raman signatures of SO_4^{2-} and S_8 respectively, and reported on Figure 3b. Contrary to the expected Gaussian distribution of the products around the point B (initial 325-nm laser focalisation), sulphur and sulphate species were heterogeneously and randomly distributed within the particle. Under photolysis with the 325-nm laser, particle was not completely immobilized do to the radial forces induced probably by the high photon flux density of the laser beam which produce a rapid photodegradation of the particle. The Δx and Δy are estimated to be ~20 µm from the high-speed video camera. The instability of the droplet under the laser beam at 325-nm induced some inhomogeneous irradiation of the droplet which would explained the random chemical heterogeneity. On contrary, the particle is stable under the Raman probe laser (633 nm) which does not produce photodegradation and enables spatially-resolved Raman analysis. Additionally, we cannot ensure that the Z-focalisation is on the same position from one point to another. Thus, the volume probed can vary and the SO_4^{2-}/S_8 ratio may change. Finally, optical images revealed the size and the appearance of the particle as a function of irradiation time. The particle, initially transparent, turned opaque during the photolysis, and its size was reduced of about 20%.

As summarised, elemental sulphur was formed in both irradiation experiments and no additional product was detected in condensed phase when a single droplet was irradiated. The formation of sulphate ions occurred only when irradiating with a 325-nm laser beam i.e. when high energy was provided to the particle.

The formation mechanism of elemental sulphur within aerosols is still not well described.[11] Photochemical generation of S_8 has been previously attributed to the photolysis of sulphur gases (SO_2, SO, H_2S) with UV light (λ< 220 nm) in anoxic environments.[30-31] Recently, we demonstrated that the UV–vis broadband photolysis of MTG in gas phase leads to $CH_3OC(O)CH_3$ and S_8 in absence of O_2.[16] In the condensed phase, the formation of reduced sulphur has been reported in anaerobic conditions and its production is promoted by microorganisms in natural environments.[32] The present work shows that elemental sulphur can be formed by photolysis of organic sulphur compound at λ> 300 nm, in the presence of oxygen with a general equation (2).

We hypothesise that the disulphide derivative was broken down to yield elemental sulphur and secondary volatile species that were quickly released into gas phase. Identification of volatile photoproducts would require further experimental investigations for analysis of gaseous phase in single droplet environment.

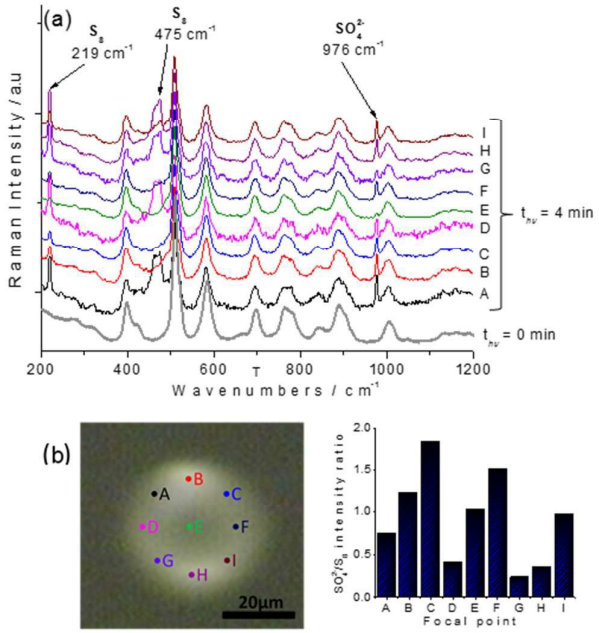

Fig. 3 Raman spectra of a levitated droplet initially containing dimethyl dithiodiglycolate (Disulphide) recorded at different location on the irradiated surface droplet. (a) before and after 4 minutes of irradiation with a 325-nm laser. Letters refer to the position of focal points. (b) Focal points of the Raman excitation beam on the particle surface and SO42-/S8 Raman band integrated intensity ratio on each focal point.

$$4\ CH_3OC(O)CH_2SSCH_2C(O)OCH_3 + h\nu \rightarrow S_8 + \text{Volatile species} \quad \text{(Eq. 2)}$$

In the atmosphere, sulphate is mainly formed from the oxidation of SO_2 by complex homogeneous and heterogeneous chemical processes.[33-35] Nonetheless, the importance of photochemical reaction, in the SO_2-to-SO_4^{2-} conversion, has already been pointed out by Cheng *et al.*[36] when the conversion rates of SO_2 to particulate sulphate was studied.

Alternatively, aqueous oxidation of natural and synthetic sulphides have been investigated due to the industrial application.[37,38] Sulphate may be produced through the general equation 3. This reaction is greatly dependent on temperature and oxygen partial pressure.

$$S + 3/2\ O_2 + H_2O \rightarrow H_2SO_4 \quad \text{(Eq. 3)}$$

View Article Online
DOI: 10.1039/C7CP08658J

In our experiments, the formation of sulphate occurred mainly through photolysis since long-term exposure of S_8-containing droplet to the humid atmosphere did not produce any sulphate ions. Thus, we propose that sulphate was formed through the photoexcitation (with the 325-nm laser) of sulphur to $S(^1D)$ state (Equation 4) followed by a quick oxidation reaction series starting from the reaction of $S(^1D)$ with oxygen to form SO_2 (Equation 5).[39] We hypothesize that all the reactions occur simultaneously on the surface of the droplet, at the gas-liquid interface, within the laser beam area penetration. The photochemical excitation of SO_2, in the 300 to 400 nm range, has been previously reported,[40] and is known to produce the singlet and triplet states of SO_2 ($^1SO_2$, $^3SO_2$) (Equation 6). It was also demonstrated that these electronic excited states reacted in the presence of O_2 and light to form SO_3, which in term formed H_2SO_4 in presence of water,[41,42] Billing et al.[43] suggested the formation of O_3 from the reaction of SO_2 with O_2, but it was not reported in other works. [44] Thus, in our experiments, SO_2, promoted by the 325-nm laser beam, is photooxidized in presence of O_2 to form SO_3 (Equation 7) and finally SO_3 reacts with water present in ambient atmosphere of the cell, to form sulphate, probably mediated by H_2SO_4 (Equation 8).

$$1/8\ S_8 + h\nu \rightarrow S(^1D) \quad \text{(Eq. 4)}$$
$$S(^1D) + O_2 \rightarrow SO_2 \quad \text{(Eq. 5)}$$
$$SO_2 + h\nu \rightarrow SO_2^* \quad \text{(Eq. 6)}$$
$$SO_2^* + O_2 \rightarrow SO_3 + O \quad \text{(Eq. 7)}$$
$$SO_3 + H_2O \rightarrow SO_4^{2-} + 2\ H^+ \quad \text{(Eq. 8)}$$

Differences between the observed products in both irradiation experiments can be explained by the higher energy and photon density provided by the laser source in comparison to the lamp. However, we cannot discard the possibility that sulphate may be formed with longer broadband light exposition under ambient atmosphere conditions.

MTG aqueous droplets. In order to evaluate the process on water-containing droplet, a fresh 0.3 M aqueous solution of MTG was injected in the acoustic cavity. A droplet of around 35 µm of diameter was trapped and a constant relative humidity (RH = 80%) kept in the levitation cell during the whole experiment time. Before irradiation, Raman spectra showed only the presence of DMTG. Disulphide was subsequently formed in a very short time in levitation compared to the pure MTG experiment.

The droplet was illuminated by a Hg-Xe lamp ($300 \leq \lambda \leq 800$ nm) through a quartz windows. As shown in Figure 4, after 70 minutes of irradiation, only elemental sulphur (α-S_8) was evidenced in the Raman spectra. As observed previously, S_8 seemed to be preferentially distributed on the particle surface. This result agreed with the hygrophobic properties of S_8 that resulted in demixing phases. Sulphate ions were not observed during these experiments. It appeared that water slowed down the photodegradation of DMTG (reaction rate coefficient k_3 near to 3.6 10^{-3} $min^{-1}$and and τ= 277.7 min) but did not prevent elemental sulphur formation. The size of the particle decreased by 22% as observed previously and the particle turned opaque. A long exposure to UV-Vis light up to 90 minutes produced strong fluorescence background in the Raman spectra that prevents the detection of products.

The aqueous-DMTG and pure DMTG photodegradation processes appeared to be similar in primary irradiation time with the formation of S_8 in condensed phase. However, long exposure time to the UV-light lead to the formation of additional secondary species that have induced florescence effect hindering the secondary products detection.

3.2. Bulk experiments

Pure MTG. 1 mL of pure MTG, placed into a closed quartz cell, was first saturated with O_2 by bubbling it into the sample for 4.5 hours. Raman spectra of the sample did not show any change during exposition to O_2 in bulk. A mixture of O_2/H_2O was also bubbled for 2 hours without evidence of disulphide derivative formation. Then, the sample was illuminated with a broadband UV-Vis light ($300 \leq \lambda \leq 800$ nm) for 48 h under constant stirring and under O_2 atmosphere. DMTG was formed from the first minutes of irradiation, identified by the S-S stretching mode near to 510 cm^{-1}. After two hours of the irradiation processes, the band attributed to elemental sulphur (S_8) appeared on the spectra accompanied by two new bands centred at 642 and 847 cm^{-1}. These two signatures were identified respectively as the OCO bending mode and the CC stretching mode of methyl acetate, MA, ($CH_3OC(O)CH_3$).[45] The other characteristic bands of MA were overlapped by MTG bands (FigureS3 of the Supporting Information).

We also performed the same experiments without bubbling O_2 into the sample. The three products namely DMTG, MA and S_8 were formed from the first minutes of irradiation. Additionally, formation of DMTG and MA were more than four times slower than experiments in presence of O_2 (see Figure S4 and Table S1 in the Supporting information section). Obviously, O_2 promotes the phototransformation of MTG into DMTG, MA and S_8 in bulk conditions (Table 1).

The normalised Raman intensities of MA and DMTG were plotted against the irradiation time on Figure 5. Unlike the linear formation of MA with the irradiation time, DMTG formation curve showed a multistep feature that could be associated to different formation channels as well as a simultaneous formation-degradation process of the disulphide. Photodegradation of MTG corresponds to a first order kinetics. Table 1 gives the reaction rate coefficients, the half-lives and the lifetimes obtained in the photodegradation of MTG in bulk conditions. It worth mentioning that the lifetime estimated from the bulk experiments (τ > 12h) are not atmospherically relevant.

Accordingly, elemental sulphur and methyl acetate were directly formed by desulphurization of MTG (Equation 9). Concurrently, formation of disulphide in this experiment seemed to be stimulated by light, contrary to the levitation experiments where it is spontaneously formed by exposition to ambient air in dark conditions. Thus, the surface of the droplet could have played an important role in the reactivity of MTG,

View Article Online
DOI: 10.1039/C7CP08658J

promoting its oxidation and formation of the disulphide derivative. Controversially, methyl acetate was not detected into the droplet while this was the main product detected into the bulk. We assumed that MA is preferentially formed from MTG and not from DMTG that is the starting species in levitation.

Transformation of MTG into DMTG could proceed via two channels: one in presence of oxygen and stimulated by light (Equation 10), and the other without participation of O_2 (Equation 11). Our results did not distinguish between the two channels.

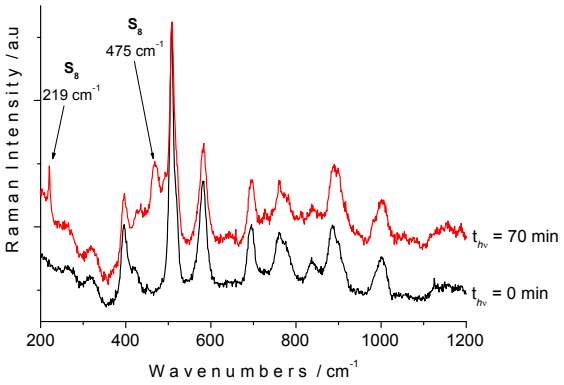

Fig. 4 Raman spectra of a levitated droplet initially containing aqueous solution of dimethyl dithiodiglycolate (disulphide) in the region of 200-1200 cm^{-1} before and after 70 minutes of irradiation with broadband UV-Vis light (300-800 nm)

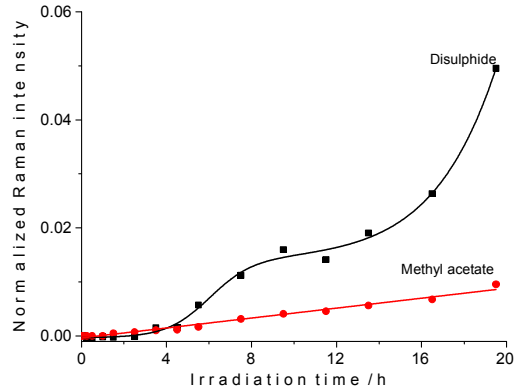

Fig. 5 Plots as a function of irradiation time of the Raman intensities of the bands assigned to dimethyl dithiodiglycolate (disulphide) and methyl acetate produced after irradiation of methyl thioglycolate in bulk in absence of O2.

$CH_3OC(O)CH_2SH + h\nu \rightarrow CH_3OC(O)CH_3 + S^{\bullet}$ (Eq. 9)

$4\ CH_3OC(O)CH_2SH + O_2 + h\nu \rightarrow 2\ [CH_3OC(O)CH_2S]_2 + 2\ H_2O$ (Eq.10)

$2\ CH_3OC(O)CH_2SH + h\nu \rightarrow [CH_3OC(O)CH_2S]_2 + H_2$ (Eq. 11)

MTG aqueous solution. A 0.3 M solution of MTG, placed into a closed quartz cell, was illuminated with a broadband UV-Vis light by a Hg-Xe lamp ($300 \leq \lambda \leq 800$ nm) for 32 h. Raman signatures of MTG were observed to disappear while new bands were growing with irradiation time. The same products as the previous pure MTG experiments i.e. DMTG, MA, and S_8 (see Figure S5 of the Supporting Information) were observed. The photodegradation was promoted by water (Table 1). Indeed, the formation of methyl acetate is twice faster in aqueous medium than pure MTG in presence of O_2 and nine times faster than in absence of O_2 (see Table S1 in the Supporting information section). DMTG and partially MA were photodegraded after 32 h of irradiation. Only S_8 and some MA dominated the Raman spectrum after 32h of irradiation.

Table 1. Reaction rate coefficients (k), half-lives ($t_{1/2}$) and lifetimes (τ) in the photodegradation of MTG with broadband UV-Vis light (300-800 nm) in bulk.

Bulk experiment	k (h^{-1})	$t_{1/2}$ (h)	τ (h)
MTG/H_2O solution	$6.92\ 10^{-2}$	10.0	14.5
Pure MTG + O_2	$4.95\ 10^{-2}$	14.0	20.2
Pure MTG	$3.40\ 10^{-2}$	20.4	29.4

Accordingly, in bulk conditions, MTG was not oxidised in the dark even when exposed to oxygen. However, exposure to the light produced the disulphide derivative, methyl acetate and S_8. Water and oxygen promoted the photodegradation process and increased the yields of the products. Methyl acetate was especially favoured in aqueous solution, while disulphide formation was increased with the presence of oxygen.

3.3. Air/aqueous interface experiments

Finally, complementary air aqueous interface experiments were conducted and these results are presented in the Supporting Information section.

The formation of MA in the gas phase from the interface was ascertained confirming the bulk experiments. Additional, product Methanethioic acid (CH_2OS) was also detected and would be the only secondary product originated from the interface irradiation since it was not detected neither in gas phase nor in condensed phase.

4. Conclusions

Photochemistry of pure and aqueous solutions of MTG was carried out by means of complementary approaches: on acoustically levitated single droplets, in bulk and air-aqueous interface conditions. Reactivity of MTG was significantly different in all experiments. In levitation, droplet surface showed to play an important role in the activation of the oxidation reaction of MTG to form the disulphide derivative –DMTG–, which is produced without irradiation. This dark oxidation is promoted in water solution. Generally, reactions occurring on levitated droplets were faster than in bulk experiments. In bulk conditions, oxidation of MTG was not

View Article Online
DOI: 10.1039/C7CP08658J

spontaneous and stimulation by light was needed. Hence, photochemistry on levitated droplets was triggered by DMTG, whereas bulk photochemical experiments were initiated from MTG, which produced an additional species, the methyl acetate that was not observed in the levitated droplets.

Irradiation of levitated single droplets containing DMTG produced mainly S_8 distributed over the droplet surface when irradiating with a broadband UV-Vis light. Formation of S_8 and SO_4^{2-} distributed in the droplet occurred with 325-nm monochromatic irradiation. Additional energy is thus required for the formation of sulphate. We propose that sulphate is formed at the surface of the droplet, as a consequence of $S(^1D)$ excited state atom generation, through photoexcitation of S_8 (at 325 nm). At the gas-liquid interface, a quick oxidation reactions of $S(^1D)$ with oxygen promoted by the light occurred and formed SO_2. The reaction between SO_2, oxygen and water lead to the sulphate formation. Irradiation with broadband light of aqueous droplets of DMTG formed a S_8 layer, which passivated the droplet surface and stopped further photodegradation of the DMTG in the core. In the broadband irradiation conditions, the reactions occurred with a lifetime which is atmospherically relevant.

Broadband irradiation of pure and aqueous MTG in bulk produced DMTG, S_8 and MA. Photodegradation of MTG is favoured in aqueous solution. The presence of O_2 enhanced the formation of DMTG and MA. In addition, MA yield strongly increased in aqueous solution.

Photochemistry at the gas-liquid interface allowed knowing the species produced in gas phase from irradiation of liquid MTG. These products could be comparable to the bulk experiments where oxidation did not happen in dark. The formation of methyl acetate is confirmed. Methanethioic acid is the only identified product that likely result from the irradiation of interface. Despite levitation photochemical experiments started from DMTG, gas phase products should be similar, except for methyl acetate and thiols, which are probably formed only from MTG.

The results obtained in this work show that elemental sulphur and in a lesser extent, sulphate can be formed directly on the droplet surface by photolysis (λ> 300 nm) of MTG, a proxy for organosulphur containing aerosol in the presence of gaseous oxygen and water. Firstly, this could be an underestimated source of sulphur-rich particles in the atmosphere, and secondly, the presence of a thin sulphur layer on particle surface would likely modify physical and chemical properties of the droplets. However, we have demonstrated that the photochemical process is complex and would require further investigation to elucidate the full mechanism. Finally, we have confirmed that single particle investigation is of prime importance for aerosol (photo)reactivity studies in laboratory because it delivers more realistic results. Regarding the atmospheric relevance, the photoreaction is more likely at the particle scale and cannot be simulated by bulk experiments.

Acknowledgements

This work was supported by funds from the "Laboratoire d'Excellence, Labex CaPPA “Chemical & Physical Properties of the Atmosphere” (WP-2), IRENI program, ECOS-MinCyT (N°A13E05) and the CPER research project CLIMIBIO. The CaPPA project (Chemical and Physical Properties of the Atmosphere) is funded by the French National Research Agency (ANR) through the PIA (Programme d'Investissement d'Avenir) under contract "ANR-11-LABX-0005-01”

Conflicts of interest

There are no conflicts of interest to declare

References

1 B. J. Finlayson-Pitts. *Farad. Disc.,*2017,**200**, 11–58.
2 J. L. Jimenez, M. R. Canagaratna, N. M. Donahue, A. S. H. Prevot, Q. Zhang, J. H. Kroll, P. F. DeCarlo, J. D. Allan, H. Coe, N. L. Ng, A. C. Aiken, K. S. Docherty, I. M. Ulbrich, A. P. Grieshop, A. L. Robinson, J. Duplissy, J. D. Smith, K. R. Wilson, V. A. Lanz, C. Hueglin, Y. L. Sun, J. Tian, A. Laaksonen, T. Raatikainen, J. Rautiainen, P. Vaattovaara, M. Ehn, M. Kulmala, J. M. Tomlinson, D. R. Collins, M. J. Cubison, E., J. Dunlea, J. A. Huffman, T. B. Onasch, M. R. Alfarra, P. I. Williams, K. Bower, Y. Kondo, J. Schneider, F. Drewnick, S. Borrmann, S. Weimer, K. Demerjian, D. Salcedo, L. Cottrell, R. Griffin, A. Takami, T. Miyoshi, S. Hatakeyama, A. Shimono, J. Y Sun, Y. M. Zhang, K. Dzepina, J. R. Kimmel, D. Sueper, J. T. Jayne, S. C. Herndon, A. M. Trimborn, L. R. Williams, E. C. Wood, A. M. Middlebrook, C. E. Kolb, U. Baltensperger, D. R. Worsnop. *Science*, 2009, **326**, 1525-1529.
3 C. A. McLinden, V. Fioletov, M. W. Shephard, N. Krotkov, C. Li, R. V. Martin, M. D. Moran, J. Joiner. *Nature Geosci.,* 2016, **9**, 496–500.
4 M. O. Andreae, *Marine Chemistry* 1990, **30**, 1–29.
5 R. J. Charlson, J. E. Lovelock, M. O. Andreae, and S. G. Warren, *Nature* 1987, **6114**, 655–661.
6 C. R. Reisch, M. A. Moran and W. B. Whitman, *Front. Microbiol*., 2011, **2**, 172.
7 J. S. Dickschat, P. Rabe and C. A. Citron, *Org. Biomol. Chem*., 2015, **13**, 1954-1968.
8 M. J. E. C. van der Maarel, M. Jansen and Theo A. Hansen, *Appl. Environ. Microb*., 1995, **61**, 48-51.
9 P. T. Visscher and B. F. Taylor, *Appl. Environ. Microb*., 1994, **60**, 4617-4619.
10 K. B. Ksionzek, O. J. Lechtenfeld, S. L. McCallister, P. Schmitt-Kopplin, J. K. Geuer, W. Geibert, B. P. Koch, *Science* 2016, **28**, 456-459.
11 C. J. Gaston, H. Furutani, S. Guazzotti, K. R. Coffee, J. Jung, M. Uematsu, and K A. Prather. *Environ. Sci. Technol*., 2015, **49**, 4861-4867.
12 L. Qiao, J. Chen and X. Yang, *J. Environ. Sci.*, 2011, **23**, 51-59.
13 N. D. Sze and M. K.W. Ko, *Atm. Environ.*, 1980, **14**, 1223-1239.
14 F. Cozzi, I. Pellegrini, G. Adami, E. Reisenhofer, M. Bovenzi, and P. Barbieri, *Central Eur. J. Chem.* 2009, **7**, 395-401.
15 A. F Longo, D. J. Vine, L. E. King, M. Oakes, R. J. Weber, L. G. Huey, A. G. Russell, and E. D. Ingall. Atmos. Chem. Phys., 2016, 16, 13389-13398.
16 Y. B. Bava, L. M. Tamone, L. C. Juncal, S. Seng, Y. A. Tobón, S. Sobanska, A. L. Picone, and R. M. Romano. *J. Photochem. Photobiol. A,* 2017, **344**, 101–107.
17 Y. A. Tobon, S. Seng, L. A. Picone, Y. B. Bava, L. C. Juncal, M. Moreau, R. M. Romano, J. Barbillat, and S. Sobanska. *J. Raman Spectr.* 2017, **48**, 1135–1137.

View Article Online
DOI: 10.1039/C7CP08658J

18 H. Chen, J. G. Navea, M. A. Young and V. H. Grassian, *J. Phys. Chem. A*, 2011, **115**, 490-499.
19 A. Gankanda and V. H. Grassian, *J. Phys. Chem. C*, 2014, **118**, 29117-29125.
20 A. P. Ault, R. C. Moffet, J. Baltrusaitis, D. B. Collins, M. J. Ruppel, L. A. Cuadra-Rodriguez, D. Zhao, T. L. Guasco, C. J. Ebben, F. M. Geiger, T. H. Bertram, K. A. Prather and V. H. Grassian, *Environ. Sci. Technol.*, 2013, **47**, 5603-5612.
21 A. P. Ault, T. L. Guasco, J. Baltrusaitis, O. S. Ryder, J. V. Trueblood, D. B. Collins, M. J. Ruppel, L. A. Cuadra-Rodriguez, K. A. Prather and V. H. Grassian, *J. Phys. Chem. Lett.*, 2014, **5**, 2493-2500.
22 A. P. Ault, T. L. Guasco, O. S. Ryder, J. Baltrusaitis, L. A. Cuadra-Rodriguez, D. B. Collins, M. J. Ruppel, T. H. Bertram, K. A. Prather and V. H. Grassian, *J. Am. Chem. Soc.*, 2013, **135**, 14528-14531.
23 L. Cappellin, T. Karl, M. Probst, O. Ismailova, P. M. Winkler, C. Soukoulis, E. Aprea, T. D. Märk, F.Gasperi, and F. Biasioli. *Environ. Sci. Tech.,* 2012, **46**, 2283-2290.
24 R. Das and S. Chattopadhyay, *Indian J. Pure Appl. Phys.*, 1978, **16**, 482-485.
25 Y. B. Bava, L. M. Tamone, L. C. Juncal, S. Seng, Y. A. Tobón, S. Sobanska, A. L. Picone and R. M. Romano, *Journal of Molecular Structure*, 2017, **1139**, 160-165.
26 L. C. Juncal, Y. B. Bava, L. M. Tamone, S. Seng, Y. A. Tobón, S. Sobanska, A. L. Picone and R. M. Romano, *Journal of Molecular Structure*, 2017, **1137**, 524-529.
27 B. Meyer, *Chemical Reviews*, 1976, **76**, 367-388.
28 A. T. Ward, *J. Phys. Chem*., 1968, **72**, 744-746.
29 B. Meyer, M. Ospina and L. B. Peter, *Anal. Chim. Acta*, 1980, **117**, 301-311
30 J. Farquhar, J. Savarino, S. Airieau, and M. H. Thiemens. *J. Geophys. Res.: Planets* 2001, **106**, 32829-32839.
31 R. Hu, S. Seager, and W. Bains. *Astrophysi. J.* 2013, **769**, 6.
32 A. Jasińska, D. Burska, J. Bolałek. *Oceanol. Hydrobiol. Stud.*, 2012. **41,** 72-82.
33 W. R. Stockwell, and J. G. Calvert, Atm. Environ. 1983, 17, 2231–2235.
34 M. A. Blitz, K. J. Hughes, and M. J. Pilling. J. Phys. Chem. A , 2003, 107, 1971–1978.
35 S.E. Schwartz, 1987 "Aqueous-phase reactions in clouds." In John, R.W. and Gordon, G.E. American chemical society, symposium series, the chemistry of acid rain: source and atmospheric processes, Washington, D.C.
36 L. Cheng, E. Peake, and A. Davis. *JAPCA* 1987, **37**, 163–167.
37 J.P. Corriou, T. Kikindai. '*Bull. Soc. chim. Fr. Partie I,* 1979, **7–8**, 247–53.
38 F. Habashi, E. L. Bauer, Ind. Eng. Chem. Fundamen. 1969, **5**, 469-471.
39 P. J. Crutzen, *Geophys. Res. Lett.* 1976, **3**, 73–76.
40 M. Bufalini, *Environ. Sci. Tech.* 1971, **5**, 685-700.
41 E. R. Gerhard, H. F. Johnstone, *Ind. Eng. Chem*. 1955 **47**, 972-976.
42 T. N. Rao, S. S. Collier, J. G. Calvert, *J. Am. Chem. Soc*. 1969, **91**, 1616-1621.
43 C. E Billings, A. W. Berger, R. Dennis, J. Driscoll, D. Lull and P. Warneck, Study of Reactions of Sulfur in Stack Plumes. Contract No. PH-86-67-125, GCA Corp., Bedford, Mass., First Annual Report, (1968)
44 D. S. Sethi, J. Air Pollut. Control Assoc. 1971, 21, 418-420.
45 J. K. Wilmshurst. *J. Molec. Spectr.* 1957, **1**, 201-215.

View Article Online
DOI: 10.1039/C7CP08658J

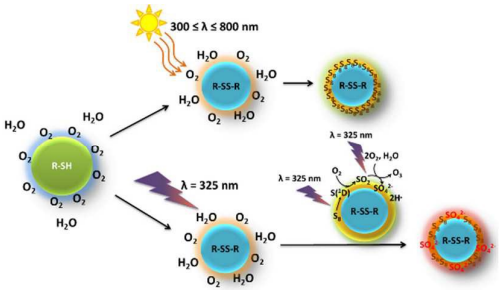

Photochemical generation of elemental sulphur and sulphate at the gas-liquid interface by heterogeneous interaction with gaseous O_2 and H_2O.